

Full length article

Formation of extended prismatic dislocation structures under indentation

J. Gagel^a, D. Weygand^{a,*}, P. Gumbsch^{a,b}^a KIT, Institute of Applied Materials, Engelbert-Arnold Str. 4, 76131 Karlsruhe, Germany^b Fraunhofer IWM, Wöhlerstr. 11, 79108 Freiburg, Germany

ARTICLE INFO

Article history:

Received 25 February 2016

Received in revised form

1 April 2016

Accepted 3 April 2016

Keywords:

Prismatic loop

Dislocation

Cross-slip

Nucleation

Indentation

Discrete dislocation dynamics

ABSTRACT

Prismatic dislocation structures are often observed after indentation experiments. These structures usually start from the zone of high dislocation density underneath an indenter tip, but extend far beyond. Three dimensional Discrete Dislocation Dynamics simulations show how these complex structures can be formed from preexisting dislocations. The specifics of the indentation stress field and the crystallographic orientation play an important role for the formation of these structures. The mechanism of formation of the prismatic dislocations loops is dominated by stress controlled cross slip events, with cross slip locations reflecting the symmetry of the indentation stress field.

© 2016 Acta Materialia Inc. Published by Elsevier Ltd. All rights reserved.

1. Introduction

Nanoindentation is a common tool not only to characterize mechanical properties of materials like hardness or elastic response at high spatial resolution, but also to gain insight into incipient plastic deformation. Such plastic deformation plays an important role for contact formation and evolution under tribological loading [1]. During loading, material below the indenter tip initially deforms elastically. The transition to the plastic regime is often associated with a pop-in: a jump in the force-displacement curve, which can be attributed to dislocation nucleation [2,3]. However, some dislocation activity has been reported even before the pop-in [4,5], which indicates, that the first pop-in is due to a heterogeneous process like the activation of a dislocation source [6]. Below the indenter tip, a zone of high dislocation density is often surrounded by a zone of lower dislocation density [7,8].

In the case of a well annealed crystal, the dislocations spreading out of the indentation zone often leave characteristic slip lines or dislocation structures that can be revealed by etch pits [9]. From the

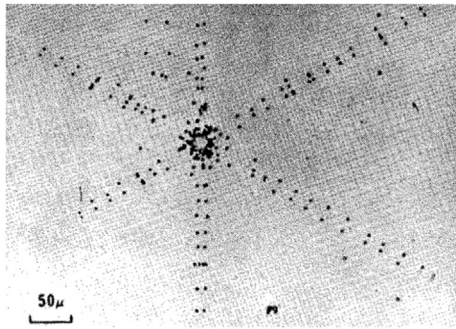
zone of high dislocation density, prismatic dislocation loops and helical prismatic dislocation structures, as well as long dislocations, can be emitted into the bulk [8].

For indentation along the [111] direction, long range dislocation rosettes have ubiquitously been observed in fcc metals like Ag [9,10], Au [11], Cu [12,13] and fcc Fe [14]. These dislocation rosettes consist of dislocation structures extending along the (110) Burgers vector directions parallel to the surface, forming six ‘arms’ [12] (Fig. 1(a)).

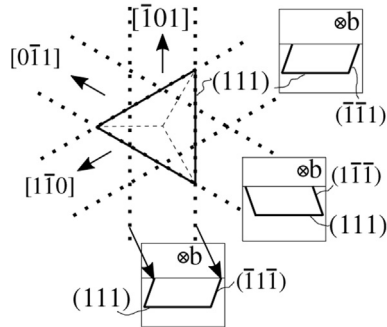
These arms are long compared to the diameter of the zone of high dislocation density underneath the indenter (Fig. 1(a)). Each arm consist of prismatic dislocation half loops (‘u-shaped’ loops) spreading out from the zone below the indenter tip [9,11,13] (Fig. 1(b)). An overview of experiments with dislocation rosettes is given in Ref. [15]. Dislocation rosettes have been observed for small loads [9,10] well below the forces needed for massive dislocation multiplication underneath the indenter. Well formed rosettes are observed for crystals with an initially low dislocation density of the order of 10^7 m^{-2} [12,13], where blocking of dislocations by forest dislocations is unlikely. Formation of fully formed dislocation rosettes is hindered by obstacles like other rosettes, subgrain boundaries or strain concentrations [9]. Occasionally, some arms of the dislocation rosettes are missing [16].

* Corresponding author.

E-mail addresses: johanna.gagel@kit.edu (J. Gagel), Daniel.Weygand@kit.edu (D. Weygand).



(a) dislocation rosette in Cu (from [12])



(b) prismatic dislocation half loops

Fig. 1. (a) Etched copper surface with [111] normal and indentation along the normal direction (reprinted with permission from Ref. [12]. Copyright 1972, AIP Publishing LLC). Dislocation rosettes consist of prismatic half loops spreading out from a zone of high dislocation density. One pair of etch pits belongs to one prismatic half loop. (b) Schematic drawing of a dislocation rosette with a Thompson Tetrahedron (adapted from Ref. [9]). Viewed in direction of the Burgers vector \mathbf{b} , dislocation half loops appear as 'u-shaped'.

Up to now, it is not well understood how such (helical) prismatic dislocation structures are generated and why, in some cases, they form characteristic rosettes. Proposed formation mechanisms of prismatic loops involve either complex reactions between several dislocations on different slip planes, or a single dislocation loop wrapping itself around a prism by multiple cross-slip and finally reacting with itself [17].

Nucleation of prismatic loops has been observed in combination with strain concentrations [16], e.g. at precipitates [18,19], at voids [20] or in metal matrix composites due to thermal stresses [21,22].

Nucleation from surface steps during nano-indentation was investigated by atomistic simulations, showing the formation of prismatic loops due to reactions between freshly nucleated dislocations [23,24]. For initially flat surfaces, atomistic simulations describe the formation of prismatic dislocation loops via homogeneously nucleated glide loops, which react with each other to form prismatic dislocation loops [25–28]. Based on such observations, prismatic dislocation loops have been implemented as a nucleation criterion in a Discrete Dislocation Dynamics (DDD) framework [7,27]. More recently, another formation mechanism for prismatic dislocation loops during indentation has been found in atomistic simulations [29,30]. At first a twin nucleates and transforms into a shear loop [29,30]. Such a shear loops can cross slip and pinch out a prismatic dislocation loop [29,30].

In this work, we do not implement such nucleation criteria, but study dislocation multiplication from preexisting dislocations underneath a spherical indenter. For scales exceeding the atomistically studied cases, the formation of extended prismatic dislocation structures is analysed.

2. Discrete Dislocation Dynamics

The 3D DDD framework is adapted from Refs. [31,32] to handle an indentation problem in a finite elastic volume. The elastic problem is solved by Finite Element (FE) simulation. More details on the DDD framework are given in Refs. [31–33]. Within the DDD framework, full dislocations are modelled as discrete lines, which are represented by a sequence of straight dislocation segments of arbitrary orientation. Only conservative dislocation motion is considered. The dislocation driving force is given by the resolved Peach-Koehler force F_{PK} on the slip plane

$$F_{PK} = (\boldsymbol{\sigma}\mathbf{n}) \cdot \mathbf{b} \quad (1)$$

with the local stress tensor $\boldsymbol{\sigma}$, the slip plane normal \mathbf{n} and the Burgers vector \mathbf{b} . A second order equation of motion is solved for the local dislocation velocity as described in Refs. [34,35].

Cross slip of screw dislocations is enabled by a statistical model [36]. The cross slip probability P per time step is

$$P = A \frac{l}{l_0} \delta t \cdot \exp\left(\frac{V(\tau - \tau_{III})}{kT}\right) \quad (2)$$

with a numerical coefficient A , the length of the screw dislocation section l , a reference length l_0 , time step δt , the activation volume for cross slip V the resolved shear stress in the cross slip plane τ , the critical resolved shear stress τ_{III} , controlling stage III hardening, the Boltzmann constant k and the absolute temperature T [36]. To avoid rapid cross slip back and forth between two planes due to local fluctuations, cross slip events are only allowed if the resolved shear stress on the cross slip plane exceeds the resolved shear stress on the glide plane by at least 10%, following [36].

The simulated samples are cuboids with outer dimensions of $3 \times 3 \times 3 \mu\text{m}^3$ or $4.8 \times 1.2 \times 2.4 \mu\text{m}^3$. Samples are discretised by $64 \times 64 \times 64$ or $128 \times 32 \times 64$ elements respectively, to represent the indenter stress field with a high spatial resolution. The displacement of the bottom surface ($y = 0$) is set to zero. Apart from the nodes within the indentation contact area, all remaining nodes at the surface and particularly at the side surfaces are traction free. A rigid spherical indenter tip with radius R is pressed into the material with a force F parallel to the negative y -axis of the laboratory coordinate system. The contact is modelled as a Hertzian contact which gives a contact radius r_c

$$r_c = \sqrt[3]{\frac{3FR}{8G}(1-\nu)} \quad (3)$$

with Poisson's ratio ν and shear modulus G of the elastic material [37]. Small strain is assumed and therefore no coupling between surface deformation due to emerging dislocations and contact radius is taken into account – the indenter force is always applied on the undeformed, flat surface. The contact between the sample surface and the indenter is modelled as frictionless and therefore only a surface pressure $p(r)$ [37]

$$p(r) = \begin{cases} -\frac{3}{2} \frac{F}{\pi r_c^2} \sqrt{1 - \frac{r^2}{r_c^2}} & , r \leq r_c \\ 0 & , r > r_c \end{cases} \quad (4)$$

is applied. The y -component F_A of the force due to the indenter on each FE node A on the surface within the contact radius $r \leq r_c$ is calculated by Gaussian integration on the concerned surface elements according to

Download English Version:

<https://daneshyari.com/en/article/7878435>

Download Persian Version:

<https://daneshyari.com/article/7878435>

[Daneshyari.com](https://daneshyari.com)